

# Photodissociation of trapped $\text{Rb}_2^+$ : Implications for hybrid molecular ion-atom trapping

S. Jyothi<sup>1</sup>, Tridib Ray<sup>1,2</sup>, Sourav Dutta<sup>1</sup>, A.R. Allouche<sup>3</sup>, Romain Vexiau<sup>4</sup>, Olivier Dulieu<sup>4</sup> and S. A. Rangwala<sup>1</sup>

<sup>1</sup>Raman Research Institute, C. V. Raman Avenue, Sadashivanagar, Bangalore 560080, India.

<sup>2</sup>Light-Matter Interactions Unit, Okinawa Institute of Science and Technology Graduate University, Onna, Okinawa 904-495, Japan.

<sup>3</sup>Institut Lumière Matière, UMR5306 Université Lyon 1 - CNRS, Université de Lyon, 69622 Villeurbanne Cedex, France.

<sup>4</sup>Laboratoire Aimé Cotton, CNRS, Université Paris-Sud, ENS Cachan, Université Paris-Saclay, Orsay Cedex, France.

We observe direct photodissociation of trapped  $^{85}\text{Rb}_2^+$  molecular ions in the presence of cooling light for the  $^{85}\text{Rb}$  magneto optical trap (MOT). Vibrationally excited  $\text{Rb}_2^+$  ions are created by photoionization of  $\text{Rb}_2$  molecules formed photoassociatively in the rubidium (Rb) MOT and are trapped in a modified spherical Paul trap co-centric with the MOT. The decay rate of the trapped  $\text{Rb}_2^+$  ion signal in the presence of the MOT cooling light is measured and agreement with our calculated rates for molecular ion photodissociation is established. The photodissociation mechanism due to the MOT light is expected to be active and therefore universal for all homonuclear diatomic alkali metal molecular ions.

PACS numbers:

Keywords:

The spatially overlapped trapping of cold atoms and ions [1–7] has significantly expanded our ability to study interactions in cold, dilute gas ensembles. In particular, atomic ion-atom collisions, charge exchange collisions [6–10], sympathetic cooling of ions by ultracold trapped atoms [5, 10–13], three body reactions [14–16] and molecular ion formation processes [3, 17] have been investigated. Two complementary directions motivate key goals for future work, (a) the low partial wave ion-atom collisions which explores quantum scattering and many particle physics and (b), the controlled collisions between the cold molecular ions produced in the ion-atom traps with co-trapped neutral atoms and with light.

A critical question which arises is whether the molecular ions can be trapped for a substantial extent of time simultaneously with an ensemble of cold atoms in order to study the interaction between them. In this letter, we address the possibility of simultaneous trapping of  $^{85}\text{Rb}_2^+$  molecular ions with ultracold  $^{85}\text{Rb}$  atoms in a magneto optical trap (MOT). Our experimental observation shows that the cooling light for the Rb MOT leads to rapid destruction of the measured  $\text{Rb}_2^+$  ion signal. We measure the lifetime of trapped  $\text{Rb}_2^+$  in the presence of 780.2413 nm ( $\equiv 12816.54 \text{ cm}^{-1}$ ) light to be  $\sim 270$  ms. We discuss possible dissociation mechanisms and show that the experimental observation is in agreement with theoretical calculations for the photodissociation of  $\text{Rb}_2^+$  molecular ions. The observed photodissociation mechanism is expected to be universal to all diatomic homonuclear alkali molecular ions as they exhibit similar potential energy characteristics.

The experimental system consists of an ion-atom hybrid trap assembly as shown in Fig. 1. The detailed description of the experimental system can be found in earlier work [5, 18, 19]. Briefly, the hybrid trap consists of a

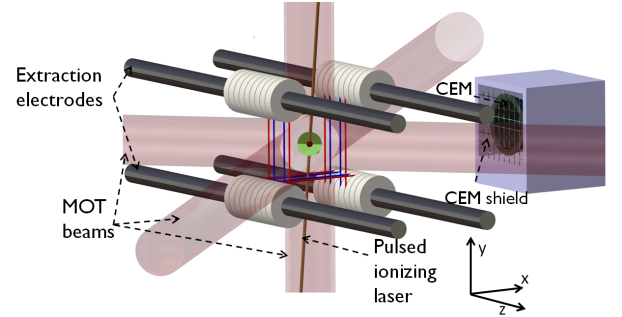


FIG. 1: Schematic of the ion-atom hybrid trap, along with a channel electron multiplier for ion detection. The outer (red) wires are the ion trap end cap electrodes and the inner (blue) wires are the rf electrodes for the ion trap. The red sphere and the green cut sphere represent the spatial extent of the MOT and the modified spherical Paul trap respectively.

MOT for atoms and a modified spherical Paul trap made of four tungsten wire loops in a square shape geometry for trapping ions. The ion trap radio frequency (rf) of 500 kHz with 150 V amplitude is applied to the inner pair of wires and a small ( $-5$  V) constant potential is applied on the outer wires. The ion trap is operated at the optimal trapping voltage for  $\text{Rb}_2^+$  ions.

For the experiment,  $^{85}\text{Rb}$  atoms are cooled and trapped in the MOT using three pairs of mutually orthogonal counter-propagating laser beams of  $\sim 8$  mm diameter intersecting at the center of a gradient magnetic field. The cooling laser beam is red detuned from the  $5S_{1/2} (F = 3) \leftrightarrow 5P_{3/2} (F' = 4)$  transition by 12 MHz. The repumper light is on resonance with the  $5S_{1/2} (F = 2) \leftrightarrow 5P_{3/2} (F' = 3)$  transition. Approximately 40 mW of cooling and 3 mW of repumper power is used and is equally distributed over the six

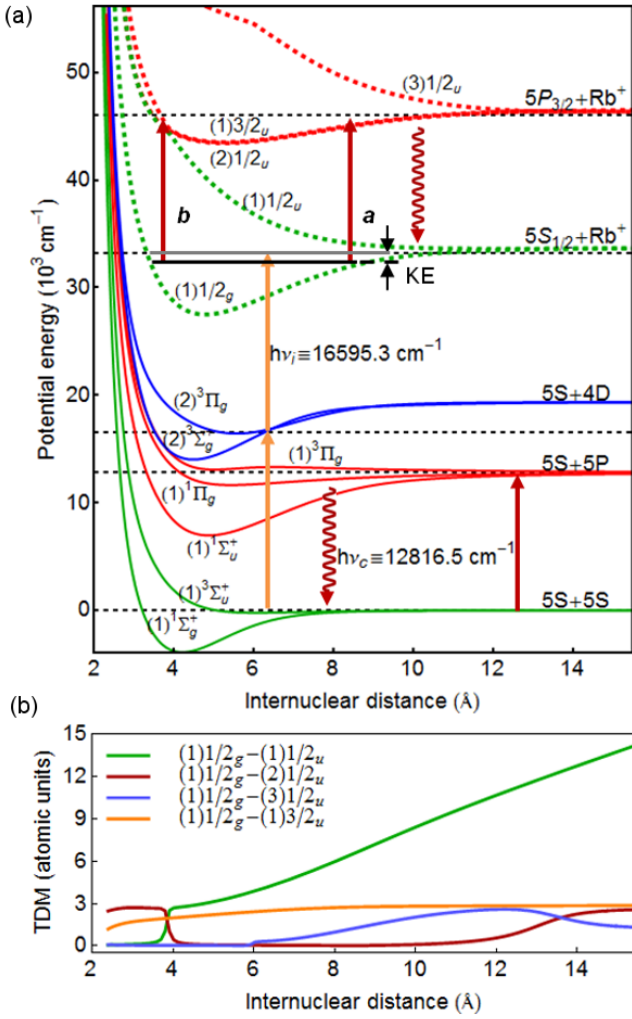


FIG. 2: Selected potential energy curves (PECs) of  $\text{Rb}_2$  and  $\text{Rb}_2^+$  molecules relevant for the experiment are shown in panel (a). The  $\text{Rb}_2^+$  PECs include spin-orbit interaction.  $\text{Rb}_2$  molecules are formed using  $12816.54 \text{ cm}^{-1}$  photons (red arrows) and are ionized using two photons of  $16595.3 \text{ cm}^{-1}$  (orange arrows) to form  $\text{Rb}_2^+$  molecules. The red arrows marked as *a* and *b* corresponds to the dissociation channels (a) and (b) described in the text. Panel (b) shows the selected transition electric dipole moments (TDM) for transitions from  $(1)1/2_g$  electronic state of  $\text{Rb}_2^+$ . The data for the plots is available in the supplementary material.

laser beams.

The  $\text{Rb}_2^+$  molecular ions are created by ionizing neutral  $\text{Rb}_2$  molecules produced by photoassociation in the MOT [20, 21]. The potential energy curves (PEC) of  $\text{Rb}_2$  [22] and  $\text{Rb}_2^+$  [23] molecules relevant for this experiment are shown in Fig. 2(a). Two Rb atoms in the ground state photoassociate in the presence of a cooling laser photon ( $h\nu_c \equiv 12816.54 \text{ cm}^{-1}$ ) to form a loosely bound molecule in the excited electronic state. The excited molecule spontaneously decays either to a highly vibrationally excited bound molecule in the electronic

ground states ( $^3\Sigma_u^+$  or  $^1\Sigma_g^+$ ) or to two free ground state atoms by emitting a photon. These loosely bound neutral  $\text{Rb}_2$  molecules are ionized by two photons of  $602.5 \text{ nm}$  ( $2h\nu_i \equiv 33190.6 \text{ cm}^{-1}$ ) to produce  $\text{Rb}_2^+$  ions in their electronic ground state  $(1)1/2_g$  (or  $X^2\Sigma_g^+$  in Hund's case "a" notation). The ionization laser is a pulsed dye laser, pumped by the second harmonic of a Nd:YAG laser (10 Hz repetition rate).

Energy consideration allows only those vibrational levels of  $\text{Rb}_2^+$  which have binding energies  $\geq 500.2 \text{ cm}^{-1}$  ( $= \text{Ionization potential}(\text{Rb}) 33690.8 \text{ cm}^{-1} - 2h\nu_i$ ) to be populated. Based on the calculation of vibrational energies [24] using the ab initio potentials [23], the vibrational level with binding energy close to  $500.2 \text{ cm}^{-1}$  is  $v=174$  of  $(1)1/2_g$  electronic state, which essentially implies that the ionization process can create  $\text{Rb}_2^+$  in levels  $v \leq 174$ . The kinetic energy (KE) of the electron determines the initial vibrational levels in which the  $\text{Rb}_2^+$  ions are created.

Since the molecular ions are created from the MOT, they are created at the centre of the ion trap. The ion trap voltages are *on* during the ionization process so that the ions are trapped as they are produced. The trapped ions are detected by extracting them onto a channel electron multiplier (CEM), by switching the voltages appropriately on a set of electrodes [5]. Prior to the extraction, the trapping rf field is switched *off* to mass separate any  $\text{Rb}^+$  ions from  $\text{Rb}_2^+$  ions [19].

The process of loading of  $\text{Rb}_2^+$  into the ion trap is monitored by extracting the ions at different times during the loading process. Fig. 3(a) shows an average of 40 such measurements. The measured rate for attaining a steady state of trapped molecular ion number is  $\sim 5.3 \text{ s}^{-1}$  and the ion trap has  $\sim 2 \text{ Rb}_2^+$  ions at steady state. The steady state is reached when the ion production rate equals the ion loss rate. In principle, the ion loss rate depends on factors such as rf heating, collisions with background gases, collisions with ultracold atoms and on the presence of light. In order to determine the dominant loss channel, we load the trap to steady state and hold the ions in the ion trap for variable hold time in different scenarios followed by ion extraction onto the CEM to count the number of ions survived.

The effect of Rb  $D_2$  light on the population of  $\text{Rb}_2^+$  molecular ions is found by measuring the lifetime of  $\text{Rb}_2^+$  when held in the presence of MOT cooling light. Each experimental cycle consists of the following sequence: loading the MOT to steady state, turning on the ion trap, turning on the pulsed dye laser to create  $\text{Rb}_2^+$ , turning off the pulsed dye laser (thus stopping further creation of  $\text{Rb}_2^+$ ), removing the MOT atoms by blocking the repump light and then holding the  $\text{Rb}_2^+$  ions in the ion trap for a predetermined holdtime either in presence or absence of the MOT cooling light. At the end of the hold time, the ions are extracted out of the ion trap and detected by the CEM. The hold time

is varied and the sequence is repeated. Fig. 3(b) shows the survival probability of  $\text{Rb}_2^+$  ions in the ion trap at different hold times either in presence (red squares) or absence (black circles) of the MOT cooling light. In the absence of MOT cooling light the lifetime of  $\text{Rb}_2^+$  ions is greater than 5 seconds while the lifetime is dramatically reduced to  $270 \pm 159$  ms in presence of the MOT cooling light.

We consider two possible channels for the disintegration of the  $\text{Rb}_2^+$  ground state molecules induced by the MOT cooling light. The dipole allowed transitions from the initial  $(1)1/2_g$  state lead to the states  $(1)1/2_u$ ,  $(2)1/2_u$ ,  $(3)1/2_u$  and  $(1)3/2_u$  (written in Hund's case c notation including spin-orbit interaction), with the relevant electric transition dipole moment (TDM) [23] shown in Fig. 2(b). Of these states, the  $(3)1/2_u$  is energetically not accessible. The  $(1)1/2_u$  state is of  $(1)^2\Sigma_u^+$

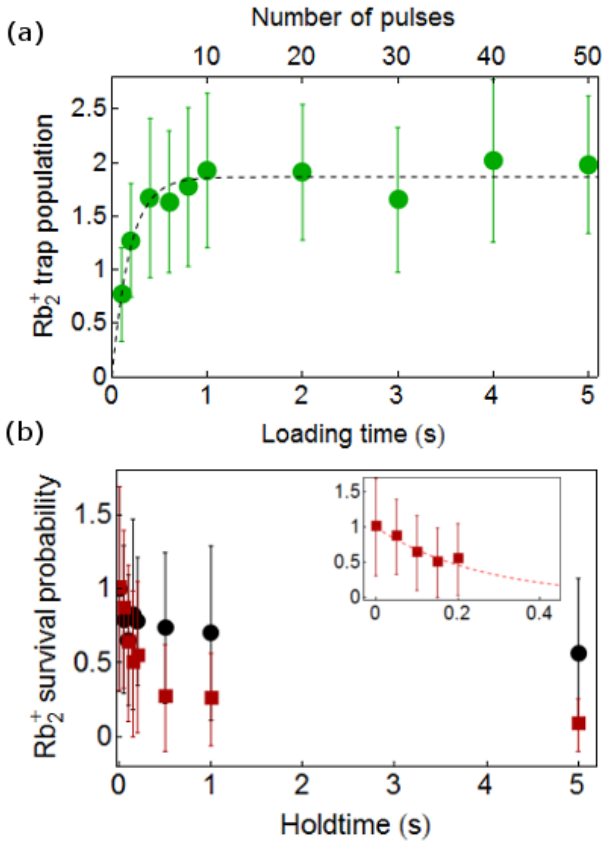
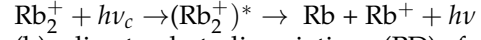


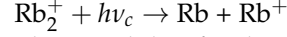
FIG. 3: Panel (a) shows the  $\text{Rb}_2^+$  ion population in the trap as a function of loading time (the top axis corresponds to the number of ionization pulses). The ion number initially increases and then saturates. The MOT trapping lasers are kept *on* during the experiment. Panel (b) shows the survival probability of  $\text{Rb}_2^+$  ions in the ion trap. The black circles represents the lifetime in the absence of MOT light fields and the red squares shows the lifetime in the presence of cooling laser field. A single exponential fit to the  $\text{Rb}_2^+$  lifetime data in the presence of cooling laser field is shown in the inset.

character beyond  $4 \text{ \AA}$ , and changes into  $(1)^2\Pi_u$  before  $4 \text{ \AA}$  due to an avoided crossing induced by the spin-orbit interaction. This explains the crossing of TDM curves in Fig. 2(b) around  $4 \text{ \AA}$ . The possible dissociation channels are shown in Fig. 2(a) and are:

(a) bound-bound excitation (indicated by *a* in Fig. 2(a)) followed by spontaneous decay to ion-atom pair.



(b) direct photodissociation (PD) from  $(1)1/2_g$  to  $(1)1/2_u$  (indicated by *b* in Fig. 2(a)).



The possibility for the dissociation of  $\text{Rb}_2^+$  ions through these excitation channels are investigated by calculating the transition rates.

In the case *a*, the energy of the cooling light  $h\nu_c$  is insufficient to excite the molecule to the continuum of the first excited electronic state (dissociation to  $5P_{1/2} + \text{Rb}^+$  asymptote). However, one can consider a resonant bound to bound transition and subsequent de-excitation to the ground state. If the de-excitation to the ground state continuum dominates over that to the bound levels, this process can be considered as a dissociation channel. We first calculate the bound-bound excitation by the MOT cooling light from various possible initial vibrational levels of the  $(1)1/2_g$  state to the  $(2)1/2_u$  and  $(1)3/2_u$  states. The accuracy of the *ab initio* PECs are not high enough to predict the vibrational levels exactly and it is thus not possible to say if the excitation is resonant or off-resonant, although the latter is more likely. Assuming resonant excitation to the nearest vibrational level determined from photon energy consideration, the maximum excitation rate is calculated to be of the order of MHz or smaller for the  $(1)1/2_g \rightarrow (1)3/2_u$  and  $(1)1/2_g \rightarrow (2)1/2_u$  transitions. The spontaneous emission rate to the bound and free states of  $(1)1/2_g$  are then calculated for both the  $(2)1/2_u$  and  $(1)3/2_u$  states. For both electronic states we find that the bound to free spontaneous emission rate is negligibly small, eliminating the possibility of this dissociation channel.

In the direct photodissociation process (case b), a bound  $\text{Rb}_2^+$  molecule in  $(1)1/2_g$  absorbs a photon  $h\nu_c$  (the slower rate determining step) to reach the  $(1)1/2_u$  state and dissociates immediately to the continuum of  $(1)1/2_u$  to form Rb and  $\text{Rb}^+$  as shown in Fig. 4(a). The photodissociation cross section  $\sigma_{pd}$  is proportional to the photon energy and the Franck-Condon overlap between the levels involved [25, 26]. The rate of photodissociation is given by

$$R_{pd} = \sigma_{pd} \times \mathcal{F} \quad (1)$$

$$= \frac{4\pi^2 a_0^2}{3\hbar c} \Delta E |\langle \psi_E(r) | d(r) | \psi_v(r) \rangle|^2 \frac{I}{h\nu_c} \quad (2)$$

where  $\sigma_{pd}$  is the dissociation cross section,  $\mathcal{F} = I/h\nu_c$  is the dissociating light flux,  $I$  is the intensity of the light,  $a_0$  is the Bohr radius,  $2\pi\hbar = h$  is the Planck's constant,  $c$  is the velocity of light,  $\Delta E$  is the photon energy and  $d(r)$  is the transition dipole moment between  $(1)1/2_g$

and  $(1)1/2_u$  states [23]. The continuum wavefunction  $\psi_E(r)$  is calculated using Cooley-Numerov method [27] and the bound wavefunction  $\psi_v(r)$  is calculated using LEVEL code [24].

The variations of the calculated PD rates vs the photon energy reproduce the oscillations of the initial bound wave functions, as shown for few vibrational levels in Fig. 4(b) [26, 28]. Fig. 4(c) shows the PD rate at photon energy  $12816.5 \text{ cm}^{-1}$  for all the vibrational levels of  $\text{Rb}_2^+$  ground state. The results show that molecular ions in different vibrational levels dissociate at different rates in presence of the MOT cooling light with the trend that the lower vibrational levels dissociate at faster rates.

The two limits concerning the vibrational level of the

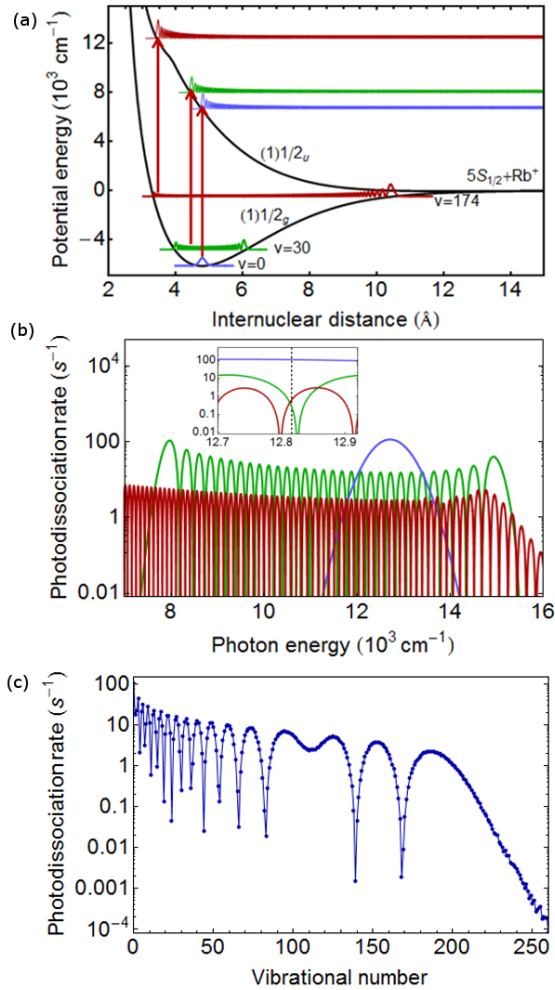


FIG. 4: Panel (a) shows the  $(1)1/2_g$  and  $(1)1/2_u$  PECs, the wavefunctions for selected vibrational levels  $v = 0$  (blue), 30 (green) and 174 (red) and the final unbound wave functions at the cooling light photon energy. Panel (b) shows the corresponding photodissociation rates as a function of the photon energy. The inset shows a zoom at energies close to  $h\nu_c$ , indicated by the vertical dashed line. In panel (c), the calculated photodissociation rate at  $h\nu_c$  is shown for all the vibrational levels of the  $(1)1/2_g$  state.

initially created  $\text{Rb}_2^+$  are determined by the KE of the ejected electron. (i) In case the electron is ejected with zero KE, the  $\text{Rb}_2^+$  ions are created in/near  $v = 174$  which dissociates at the calculated rate of  $0.7_{-0}^{+1.4} \text{ s}^{-1}$ . The systematic error bar (asymmetric) is determined by considering the uncertainty in the dissociation energy of the ab initio PEC compared to the experimental dissociation energy [29], which is higher by  $120 \text{ cm}^{-1}$ , and causes systemic shift of the calculated vibrational levels and hence the PD rates. (ii) In case of electron ejection with all possible KE, all vibrational levels of  $\text{Rb}_2^+$  from  $v = 0$  to 174 may be populated. An average of calculated PD rates (Fig. 4(c)) over all vibrational levels below  $v = 174$  yields  $5.9 \pm 9.9 \text{ s}^{-1}$ . The experimentally measured rate  $3.7 \pm 2.5 \text{ s}^{-1}$  is consistent with either of the above cases. Further detailed experimental and theoretical work is thus needed to establish the initial vibrational distribution of  $\text{Rb}_2^+$ . However, even in the absence of such information, the experimental and theoretical results presented above firmly establish that light near  $D_2$  transition induces dissociation of  $\text{Rb}_2^+$ . It should also be noted that the commonly used 1064 nm light for optical dipole trapping would dissociate loosely bound  $\text{Rb}_2^+$  ( $v > 10$ ) by a similar process but have no significant effect on deeply bound  $\text{Rb}_2^+$  (e.g.  $v = 0$ ).

The above experiments and calculations show that the direct photodissociation of  $\text{Rb}_2^+$  ion by the cooling light of the MOT is the dominant mechanism for the loss of trapped  $\text{Rb}_2^+$  molecular ions in all vibrational states. Since all homonuclear alkali (X) molecular ion dimers,  $\text{X}_2^+$ , have a similar arrangement of their molecular PECs [30], we conclude through preliminary inspection that this photodissociation process will be active and influential for all such molecular ion systems. This would imply that in the presence of the MOT cooling light, long lived trapping of  $\text{X}_2^+$  will be challenging, and creating sizable steady state ensembles of  $\text{X}_2^+$  ions and parent alkali atoms would be experimentally difficult. Finally it is worth noting that direct photodissociation in  $\text{Rb}_2^+$  demonstrated here can provide a cold gas system analogous to  $\text{H}_2^+$ . If so, then  $\text{Rb}_2^+$  and its interactions with Rb and  $\text{Rb}_2$  can provide useful insights into primordial hydrogen chemistry. Such studies might help understanding the lack of detection of  $\text{H}_2^+$  ions in interstellar medium [31] and future experiments could help in constraining the collision rates for the formation of  $\text{H}_3^+$ .

S. J. and S. A. R. acknowledge Krishna Rai Dastidar for assistance in the setting up of the molecular level calculations. S. D. acknowledges support in the form a Pancharatnam Fellowship from RRI. A. R. A. acknowledges the access to the HPC resources of the FLMSN, "Fédération Lyonnaise de Modélisation et Sciences Numériques", partner of EQUIPEX EQUIP@MESO and HPC of the "Centre de calcul CC-IN2P3" at Villeurbanne.

- 
- [1] W. W. Smith, O. P. Makarov, and J. Lin, *Journal of Modern Optics* **52**, 2253 (2005).
- [2] C. Zipkes, S. Palzer, C. Sias, and M. Köhl, *Nature* **464**, 388 (2010).
- [3] F. H. J. Hall, M. Aymar, N. Bouloufa-Maafa, O. Dulieu, and S. Willitsch, *Phys. Rev. Lett.* **107**, 243202 (2011).
- [4] K. Ravi, S. Lee, A. Sharma, G. Werth, and S. Rangwala, *Applied Physics B* **107**, 971 (2012).
- [5] T. Ray, S. Jyothi, N. Ram, and S. Rangwala, *Applied Physics B* **114**, 267 (2014).
- [6] A. T. Grier, M. Cetina, F. Oručević, and V. Vuletić, *Phys. Rev. Lett.* **102**, 223201 (2009).
- [7] W. G. Rellergert, S. T. Sullivan, S. Kotochigova, A. Petrov, K. Chen, S. J. Schowalter, and E. R. Hudson, *Phys. Rev. Lett.* **107**, 243201 (2011).
- [8] S. Lee, K. Ravi, and S. A. Rangwala, *Phys. Rev. A* **87**, 052701 (2013).
- [9] S. Haze, R. Saito, M. Fujinaga, and T. Mukaiyama, *Phys. Rev. A* **91**, 032709 (2015).
- [10] I. Sivarajah, D. S. Goodman, J. E. Wells, F. A. Narducci, and W. W. Smith, *Phys. Rev. A* **86**, 063419 (2012).
- [11] K. Ravi, S. Lee, A. Sharma, G. Werth, and S. Rangwala, *Nat Commun* **3**, 1126 (2012).
- [12] F. H. J. Hall and S. Willitsch, *Phys. Rev. Lett.* **109**, 233202 (2012).
- [13] S. Dutta, R. Sawant, and S. A. Rangwala, *arXiv:1512.04197* (2015).
- [14] A. Härter, A. Krüchow, A. Brunner, W. Schnitzler, S. Schmid, and J. Hecker Denschlag, *Phys. Rev. Lett.* **109**, 123201 (2012).
- [15] A. Härter, A. Krüchow, M. Deiß, B. Drews, E. Tiemann, and J. Hecker Denschlag, *Nat Phys* **9**, 512 (2013).
- [16] A. Krüchow, A. Mohammadi, A. Härter, J. Hecker Denschlag, J. Pérez-Ros, and C. H. Greene, *arXiv:1510.04938* (2015).
- [17] H. da Silva Jr, M. Raoult, M. Aymar, and O. Dulieu, *New Journal of Physics* **17**, 045015 (2015).
- [18] T. Ray, A. Sharma, S. Jyothi, and S. A. Rangwala, *Phys. Rev. A* **87**, 033832 (2013).
- [19] S. Jyothi, T. Ray, and S. Rangwala, *Applied Physics B* **118**, 131 (2015).
- [20] C. Gabbanini, A. Fioretti, A. Lucchesini, S. Gozzini, and M. Mazzoni, *Phys. Rev. Lett.* **84**, 2814 (2000).
- [21] A. R. L. Caires, V. A. Nascimento, D. C. J. Rezende, V. S. Bagnato, and L. G. Marcassa, *Phys. Rev. A* **71**, 043403 (2005).
- [22] A.-R. Allouche and M. Aubert-Frécon, *The Journal of Chemical Physics* **136**, 114302 (2012).
- [23] Supplementary.
- [24] R. J. L. Roy, *LEVEL 8.0: A Computer Program for Solving the Radial Schrodinger Equation for Bound and Quasibound Levels*, University of Waterloo Chemical Physics Research Report CP-663 (2007), see <http://leroy.uwaterloo.ca/programs/>.
- [25] H. Lefebvre-Brion and R. W. Field, *The Spectra and Dynamics of Diatomic Molecules* (Elsevier Academic Press, 2004).
- [26] G. H. Dunn, *Physical Review* **172**, 1 (1969).
- [27] I. N. Levine, *Quantum Chemistry* (Pearson Education Inc., New Jersey, U.S.A., 2009).
- [28] J. J. Blange, X. Urbain, H. Rudolph, H. A. Dijkerman, H. C. W. Beijerinck, and H. G. M. Heideman, *Journal of Physics B: Atomic, Molecular and Optical Physics* **29**, 2763 (1996).
- [29] M. A. Bellos, R. Carollo, J. Banerjee, M. Ascoli, A.-R. Allouche, E. E. Eyler, P. L. Gould, and W. C. Stwalley, *Phys. Rev. A* **87**, 012508 (2013).
- [30] T. E. Sharp, *At. Data* **2**, 119 (1971).
- [31] D. Galli and F. Palla, *Astron. Astrophys.* **335**, 403 (1998).